

End-to-End Transformer Based Model for Image Captioning

Yiyu Wang¹, Jungang Xu^{2*}, Yingfei Sun¹

¹School of Electronic, Electrical and Communication Engineering, University of Chinese Academy of Sciences

²School of Computer Science and Technology, University of Chinese Academy of Sciences
wangyiyu18@mails.ucas.ac.cn, xujg@ucas.ac.cn, yfsun@ucas.ac.cn

Abstract

CNN-LSTM based architectures have played an important role in image captioning, but limited by the training efficiency and expression ability, researchers began to explore the CNN-Transformer based models and achieved great success. Meanwhile, almost all recent works adopt Faster R-CNN as the backbone encoder to extract region-level features from given images. However, Faster R-CNN needs a pre-training on an additional dataset, which divides the image captioning task into two stages and limits its potential applications. In this paper, we build a pure Transformer-based model, which integrates image captioning into one stage and realizes end-to-end training. Firstly, we adopt SwinTransformer to replace Faster R-CNN as the backbone encoder to extract grid-level features from given images; Then, referring to Transformer, we build a refining encoder and a decoder. The refining encoder refines the grid features by capturing the intra-relationship between them, and the decoder decodes the refined features into captions word by word. Furthermore, in order to increase the interaction between multi-modal (vision and language) features to enhance the modeling capability, we calculate the mean pooling of grid features as the global feature, then introduce it into refining encoder to refine with grid features together, and add a pre-fusion process of refined global feature and generated words in decoder. To validate the effectiveness of our proposed model, we conduct experiments on MSCOCO dataset. The experimental results compared to existing published works demonstrate that our model achieves new state-of-the-art performances of 138.2% (single model) and 141.0% (ensemble of 4 models) CIDEr scores on 'Karpathy' offline test split and 136.0% (c5) and 138.3% (c40) CIDEr scores on the official online test server. Trained models and source code will be released.

Introduction

Image captioning aims to automatically describe the visual content of a given image with fluent and credible sentences. It is a typical multi-modal learning task, which connects Computer Vision (CV) and Natural Language Processing (NLP). Inspired by the success of deep learning methods in machine translation (Papineni et al. 2002; Cho et al. 2014), almost all image captioning models adopt the

encoder-decoder framework with the visual attention mechanism. The encoder encodes input images into fix-length vector features, and the decoder decodes image features into descriptions word by word (Vinyals et al. 2015; Xu et al. 2015; Anderson et al. 2018; Huang et al. 2019; Pan et al. 2020).

Initially, researchers adopted a pre-trained Convolutional Neural Network (CNN) as an encoder to extract image grid-level features and Recurrent Neural Network (RNN) as a decoder (Vinyals et al. 2015; Xu et al. 2015). (Anderson et al. 2018) first adopted Faster R-CNN to extract region-level features. Due to its overwhelming advantage, most subsequent works followed this pattern, and grid-level features extracted by CNN were discarded. Nevertheless, there are still some inherent defects in region-level features and encoder of object detector: 1) region-level features may not cover the entire image, which results in the lack of fine-grained information (Luo et al. 2021); 2) extracting region features is high time consuming, and the object detector needs an extra Visual Genome (Krishna et al. 2017) dataset for pre-training, which makes it difficult to train image captioning model end-to-end from image pixels to descriptions, and also limits potential applications in the actual scene (Jiang et al. 2020).

Decoder of LSTM (Hochreiter and Schmidhuber 1997) with soft attention (Xu et al. 2015) mechanism has remained the common and dominant approach in the past few years. However, the shortcomings of training efficiency and expression ability of LSTM also limit the effect of relevant models. Inspired by the success of Multi-head Self-Attention (MSA) mechanism and Transformer architecture in NLP tasks (Vaswani et al. 2017), many researchers began to introduce MSA into decoder of LSTM (Huang et al. 2019; Pan et al. 2020) or directly adopt Transformer architecture as decoder (Cornia et al. 2020; Pan et al. 2020; Luo et al. 2021; Ji et al. 2021) of image captioning models.

Especially, Transformer architecture gradually shows extraordinary potential in CV tasks (Dosovitskiy et al. 2021; Liu et al. 2021) and multi-modal tasks (Lu et al. 2019; Zhu and Yang 2020; Radford et al. 2021), which provides a new choice for encoding images into vector features. Different from Faster R-CNN, features extracted by a visual transformer are grid-level features, which have a higher computing efficiency and allows expediently exploring more effective and complex designs for image captioning.

*Corresponding Author

Considering the disadvantage of pre-trained CNN and object detector in encoder and limitations of LSTM in decoder, we build a pure Transformer-based image captioning model (PureT) to integrate this task into one stage without pre-training process of object detection to achieve end-to-end training. In Encoder, we adopt Swin-Transformer (Liu et al. 2021) to extract grid features from given images as the initial vector features and compute the average pooling of grid features as the initial image global feature. Then, we construct a refining encoder similar to (Huang et al. 2019; Cornia et al. 2020; Ji et al. 2021) by Shifted Window MSA (SW-MSA) from Swin-Transformer to refine image initial grid features and global feature. The refining encoder has a similar architecture with Transformer Encoder in machine translation (Vaswani et al. 2017) which can be regarded as an extension of Encoder of SwinTransformer for image captioning model. In Decoder, we directly adopt Transformer Decoder in machine translation (Vaswani et al. 2017) to generate captions. Furthermore, we pre-fuse the word embedding vector with the image global feature from Encoder before the MSA of word embedding vector to increase the interaction of inter-model (image-to-words) features.

We validate our model on MSCOCO (Lin et al. 2014) offline “Karpathy” (Karpathy and Fei-Fei 2017) test split and official online test server. The results demonstrate that our PureT achieves new state-of-the-art performance on both single model and ensemble of 4 models configurations: on offline “Karpathy” test split, a single model and an ensemble of 4 models achieve 138.2% and 140.8% CIDEr scores respectively; on official online test server, an ensemble of 4 models achieves 135.3% (c5) and 138.0% (c40) CIDEr.

Our main contributions are summarized as follows:

- We construct a pure Transformer-based (PureT) model for image captioning, which integrates this task into one stage again without the pre-training process of object detector and provide a new simple and solid baseline of image captioning.
- We add a pre-fusion process between the generated word embeddings and image global feature, which aims to increase the interaction of inter-modal features and enhance the reasoning ability from image to captions.
- We conduct extensive experiments on the MSCOCO dataset, which demonstrate the effectiveness of our proposed model, and achieve a new state-of-the-art performance on both ‘Karpathy’ offline test split and official online test server.

Related Work

Existing works of image captioning can be divided into CNN-LSTM based models (Vinyals et al. 2015; Xu et al. 2015; Anderson et al. 2018; Wang, Chen, and Hu 2019; Huang et al. 2019) and CNN-Transformer based models (Herdade et al. 2019; Li et al. 2019; Pan et al. 2020; Cornia et al. 2020; Ji et al. 2021; Luo et al. 2021). Both adopted pre-trained CNN or Faster R-CNN as the encoder to encode image into grid or region-level features, where the former models adopted Long Short-Term Memory Network (LSTM) (Hochreiter and Schmidhuber 1997) as the decoder and the

latter models adopted Transformer (Vaswani et al. 2017) as the decoder to generate description word by word.

Earlier works used pre-trained CNN, e.g., VGG-16 (Simonyan and Zisserman 2015) and ResNet-101 (He et al. 2016), as the encoder to encode image into grid-level features with fixed-length, and then LSTM with attention mechanism was applied among them to generate captions (Xu et al. 2015; Rennie et al. 2017). (Anderson et al. 2018) first introduced Faster R-CNN (Ren et al. 2017) into image captioning to extract the region-level features more in line with the human visual habits, which has become a typical pattern to extract image features in subsequent works.

Above all models adopted LSTM as the decoder, which have shortcomings in training efficiency and expression ability. Recently, researchers began to explore the application of transformer in image captioning. (Herdade et al. 2019) proposed the Object Relation Transformer to introduce the region spatial information. (Pan et al. 2020) proposed the X-Linear attention block to capture the 2^{nd} order interactions between the single- or multi-modal, and integrated it into the Transformer encoder and decoder. (Cornia et al. 2020) designed a mesh-like connectivity in decoder to exploit both low-level and high-level features from the encoder. (Luo et al. 2021) proposed a Dual-Level Collaborative Transformer (DLCT) to process both grid- and region-level features for realizing the complementary advantages.

Despite the outstanding performance of region-level features extracted by Faster R-CNN, the lack of fine-grained information of region-level and the time cost of Faster R-CNN pre-training are unavoidable problems. Furthermore, extracting region-level features is time-consuming, so most models directly trained and evaluated on cached features instead of image, which makes it difficult to train image captioning model end-to-end from image to descriptions.

Model

The overall architecture of our PureT model is shown in Figure 1. We adopt the widely used encoder-decoder framework, in which the encoder consists of a backbone of Swin-Transformer and stacks of N refining encoder blocks and the decoder consists of stacks of N decoder blocks. The encoder is in charge of extracting grid features from the input image and refining them by capturing the intra-relationship between them. The decoder uses the refined image grid features to generate the captions word by word by capturing the inter-relationship between word and image grid features.

Attention Mechanism

The attention mechanism can be abstractly summarized as follows:

$$\text{Attention}(q, k, v) = f_{sim}(q, k)v \quad (1)$$

where $f_{sim}(\cdot)$ is a function used to compute the similarity scores between some queries (q) and keys (k). The output of attention mechanism is the weighted sum on values (v) based on similarity scores.

In our model, Multi-head Self Attention (MSA) (Vaswani et al. 2017) and its variants Window MSA / Shifted Window

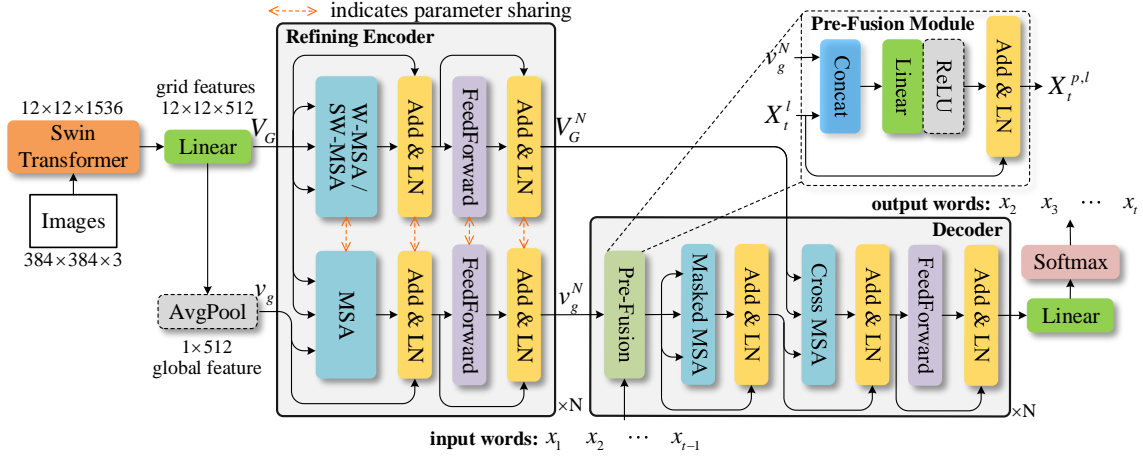


Figure 1: Overview of our proposed PureT model. We first extract image grid features V_G using SwinTransformer. v_g is calculated as the average pooling of V_G . Then V_G and v_g are refined into V_G^N and v_g^N through the Refining Encoder composed of N blocks stacks and are fed into the Decoder to generate description word by word.

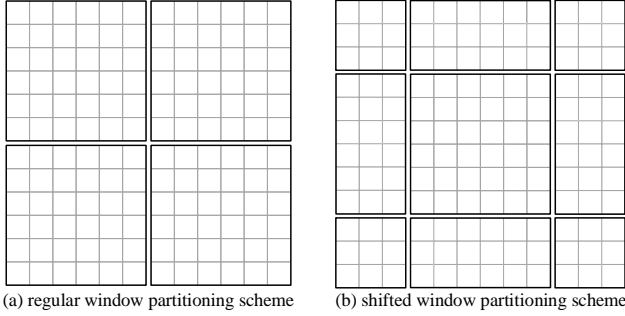


Figure 2: Illustration of regular window partitioning scheme and shifted window partitioning scheme adopted in refining encoder. The size of input feature map is $H \times W = 12 \times 12$.

MSA (W-MSA / SW-MSA) modules proposed by SwinTransformer (Liu et al. 2021) are used, where MSA is adopted in the decoder to model the intra-relationship of word sequence and the inter-relationship between word and grid features, and W-MSA / SW-MSA are adopted in the encoder to model intra-relationship of image grid features. The above three attention modules use $\text{Softmax}(\cdot)$ as the similarity scoring function, which can be formulated as follows:

$$\text{Attention}(q, k, v) = \text{Softmax}\left(\frac{qk^T}{\sqrt{d_k}}\right)v \quad (2)$$

where d_k is the dimension of k .

$$\text{MSA}(Q, K, V) = \text{Concat}(\text{head}_1, \dots, \text{head}_h) \quad (3)$$

$$\text{head}_i = \text{Attention}(Q^i, K^i, V^i), i = 1, 2, \dots, h$$

where h is the number of heads. Q^i, K^i and V^i are the i -th slice of Q, K and V respectively, which can be formulated as follows:

$$\star = \text{Concat}(\star^1, \dots, \star^i, \dots, \star^h) \quad (4)$$

where $\star \in \mathbb{R}^{L_\star \times D_\star}$ and $\star^i \in \mathbb{R}^{L_\star \times \frac{D_\star}{h}}$ (\star refers to Q, K and V), L_\star and D_\star are the length and dimension.

In the i -th head of MSA, each token of the query Q^i calculates its similarity with all tokens of the key K^i , and performs the weighted sum on all tokens of the value V^i to obtain the corresponding output. Therefore, MSA can be regarded as a global attention mechanism.

W-MSA and SW-MSA Aiming at the quadratic complexity caused by the global computation of MSA, SwinTransformer proposed W-MSA and SW-MSA to compute self-attention within local windows (Liu et al. 2021). In this paper, both W-MSA and SW-MSA are used in the encoder, in which inputs of Q, K and V are all from image grid features, therefore they have the same length $L = H \times W$ and dimension D .

Compared with MSA, W-MSA and SW-MSA first partition the inputs of Q, K and V into several windows, and then apply MSA separately in each window. Figure 2 illustrate the regular window partitioning scheme and shifted window partitioning scheme of W-MSA and SW-MSA respectively. Adding SW-MSA after W-MSA aims to solve the lack of connections across windows of W-MSA module to further improve the modeling ability. W-MSA and SW-MSA can be formulated as follows:

$$\text{(S)W-MSA}(Q, K, V) = \text{Merge}(\text{window}_1, \dots, \text{window}_w) \quad (5)$$

$$\text{window}_i = \text{MSA}(Q_W^i, K_W^i, V_W^i), i = 1, 2, \dots, w$$

where w is the number of windows and $\text{Merge}(\cdot)$ is the reverse operation of regular/shifted window partitioning scheme. Q_W^i, K_W^i and V_W^i are the i -th window of Q, K and V respectively, which can be formulated as follows:

$$\star = \text{Merge}(\star_W^1, \dots, \star_W^i, \dots, \star_W^w) \quad (6)$$

where $\star \in \mathbb{R}^{L \times D}$ and $\star_W^i \in \mathbb{R}^{\frac{L}{w} \times D}$ (\star refers to Q, K and V).

Encoder

Different from most existing models, we first employ Swin-Transformer (Liu et al. 2021) instead of pre-trained CNN or Faster R-CNN as the backbone encoder to extract a set of grid features $V_G = \{v_1, v_2, \dots, v_m\}$ from given input images as the initial visual features, where $v_i \in \mathbb{R}^D$, D is the embedding dimension of each grid feature, and m is the number of grid features ($m = 12 \times 12$ in this paper).

After grid features V_G are extracted, we refer to the standard transformer encoder (Vaswani et al. 2017) to construct a refining encoder to enhance the grid features by capturing the intra-relationship between them. Furthermore, inspired by (Ji et al. 2021), we calculate the mean pooling of grid features $v_g = \frac{1}{m} \sum_{i=1}^m v_i$ as the initial global feature and introduce it into W-MSA and SW-MSA. Specifically, when applying MSA in each window, the global feature is added into the keys k and values v as an extra token. Meanwhile, we also refine the global feature by using it as an extra query q token and applying MSA on all grid features.

As shown in Figure 1, the refining encoder is composed of N blocks stacked in sequence ($N = 3$ in this paper), and each block consists of a W-MSA or SW-MSA module with feedforward layer, in which W-MSA and SW-MSA are used alternately. The l -th block can be formulated as follows:

$$\hat{V}_G^l = \text{LayerNorm} \left(V_G^{l-1} + (\text{S})\text{W-MSA} \left(W_Q^l V_G^{l-1}, W_K^l [V_G^{l-1}; v_g^{l-1}]_s, W_V^l [V_G^{l-1}; v_g^{l-1}]_s \right) \right) \quad (7)$$

$$\hat{v}_g^l = \text{LayerNorm} \left(v_g^{l-1} + \text{MSA} \left(W_Q^l v_g^{l-1}, W_K^l [V_G^{l-1}; v_g^{l-1}]_s, W_V^l [V_G^{l-1}; v_g^{l-1}]_s \right) \right) \quad (8)$$

$$V_G^l = \text{LayerNorm} \left(\hat{V}_G^l + \text{FeedForward}(\hat{V}_G^l) \right) \quad (9)$$

$$v_g^l = \text{LayerNorm} \left(\hat{v}_g^l + \text{FeedForward}(\hat{v}_g^l) \right) \quad (10)$$

where V_G^{l-1} and v_g^{l-1} denote the output grid features and global feature of block $l-1$ respectively, and which are used as the input of block l , in which $V_G^0 = V_G$ and $v_g^0 = v_g$, $W_Q^l, W_K^l, W_V^l \in \mathbb{R}^{D \times D}$ are learnt parameter matrices; $[V_G^{l-1}; v_g^{l-1}]_s \in \mathbb{R}^{(k+1) \times D}$ denotes the stack operation of grid features and global feature and $\text{FeedForward}(\cdot)$ consists of two linear layer with ReLU activation function in between, as formulated below:

$$\text{FeedForward}(x) = W_2 \text{ReLU}(W_1 x) \quad (11)$$

where $W_1 \in \mathbb{R}^{(4D) \times D}$ and $W_2 \in \mathbb{R}^{D \times (4D)}$ are the learnt parameter matrices of two linear layers respectively. Note that the parameter of refining process for grid features and global feature are reused. The output refined grid features V_G^N and refined global feature v_g^N of block N are fed into the decoder as the input of visual content.

Decoder

The decoder aims to generate the output caption word by word conditioned on the refined global and grid features from the encoder. The interaction between multi-modal occurs in this part. As shown in Figure 1, the decoder is composed of N blocks stacked in sequence ($N = 3$ in this paper), where each block can be divided into three modules:

- 1) Pre-Fusion Module, which contains the pre-fusion process between previously generated words and refined global feature, which can be regarded as the first inter-modal interaction between natural language and visual content;
- 2) Language Masked MSA Module, which can be regarded as the intra-modal interaction within the generated words;
- 3) Cross MSA Module, which contains a MSA module with a Feed-Forward layer, which can be regarded as the second inter-modal interaction between visual content and natural language;
- 4) Word Generation Module, which contains a linear layer with softmax function.

Pre-Fusion Module Most recent Transformer-based models only use image region or grid features without global feature, where the interaction between multi-modal features only occurs in cross attention between generated word and visual features before generating the next word. The lack of interaction of global contextual information limits reasoning capability to a certain extent. Therefore, we construct a pre-fusion module to fuse the refined global feature v_g^N into the input of each block of decoder, which can be regarded as the first time multi-modal interaction to capture global visual context information and can be formulated as follows:

$$X_{1:t-1}^{p,l} = \text{Layer Norm} \left(X_{1:t-1}^{l-1} + \text{ReLU} \left(W_f [X_{1:t-1}^{l-1}; v_g^N] \right) \right) \quad (12)$$

where $X_{1:t-1}^{l-1} \in \mathbb{R}^{(t-1) \times D}$ denotes the output of block $l-1$ and is used as the input of block l at t -th timestep, $[X_{1:t-1}^{l-1}; v_g^N] \in \mathbb{R}^{(t-1) \times 2D}$ indicates concatenation and $W_f \in \mathbb{R}^{D \times 2D}$ is learnt parameters of a linear layer; the output $X_{1:t-1}^{p,l} \in \mathbb{R}^{(t-1) \times D}$ is fed into the Language Masked MSA Module. Note that the initial input at the first block comes from the previously generated words:

$$X_{1:t-1}^0 = W_e x_{1:t-1} \quad (13)$$

where $x_{1:t-1}$ are one-hot encodings of the generated words before t -th timestep, and $W_e \in \mathbb{R}^{D \times |\Sigma|}$ is the word embedding matrix of the vocabulary Σ .

Language Masked MSA Module The module aims to model the intra-modal relationship (words-to-words) within $X_{1:t-1}^{p,l}$, which can be formulated as follows:

$$\tilde{X}_{t-1}^l = \text{LayerNorm} \left(X_{t-1}^{p,l} + \text{MSA} \left(W_Q^{m,l} X_{t-1}^{p,l}, W_K^{m,l} X_{1:t-1}^{p,l}, W_V^{m,l} X_{1:t-1}^{p,l} \right) \right) \quad (14)$$

where $W_Q^{m,l}, W_K^{m,l}, W_V^{m,l} \in \mathbb{R}^{D \times D}$ are learnt parameters, and $X_{t-1}^{p,l}$ indicates the corresponding embedding vector of the generated word at $(t-1)$ -th timestep, which means that each word is only allowed to calculate attention map at its earlier generated words.

Cross MSA Module The module aims to model the inter-modal relationship (words-to-vision) between $\tilde{X}_{1:t-1}^l$ and V_G^N , which can be regarded as the second time multi-modal interaction to capture local visual context information and

Models	Single Model					Ensemble Model						
	B-1	B-4	M	R	C	S	B-1	B-4	M	R	C	S
CNN-LSTM based models												
SCST	-	34.2	26.7	55.7	114.0	-	-	35.4	27.1	56.6	117.5	-
RFNet	79.1	36.5	27.7	57.3	121.9	21.2	80.4	37.9	28.3	58.3	125.7	21.7
Up-Down	79.8	36.3	27.7	56.9	120.1	21.4	-	-	-	-	-	-
GCN-LSTM	80.5	38.2	28.5	58.3	127.6	22.0	80.9	38.3	28.6	58.5	128.7	22.1
AoANet	80.2	38.9	29.2	58.8	129.8	22.4	81.6	40.2	29.3	59.4	132.0	22.8
X-LAN	80.8	39.5	29.5	59.2	132.0	23.4	81.6	40.3	29.8	59.6	133.7	23.6
CNN-Transformer based models												
ORT	80.5	38.6	28.7	58.4	128.3	22.6	-	-	-	-	-	-
X-Transformer	80.9	39.7	29.5	59.1	132.8	23.4	81.7	40.7	29.9	59.7	135.3	23.8
\mathcal{M}^2 Transformer	80.8	39.1	29.2	58.6	131.2	22.6	82.0	40.5	29.7	59.5	134.5	23.5
RSTNet	81.8	40.1	29.8	59.5	135.6	23.3	-	-	-	-	-	-
GET	81.5	39.5	29.3	58.9	131.6	22.8	82.1	40.6	29.8	59.6	135.1	23.8
DLCT	81.4	39.8	29.5	59.1	133.8	23.0	82.2	40.8	29.9	59.8	137.5	23.3
PureT	82.1	40.9	30.2	60.1	138.2	24.2	83.4	42.1	30.4	60.8	141.0	24.3

Table 1: Offline evaluation results of our proposed model and other existing state-of-the-art models on MSCOCO ‘‘Karpathy’’ test split, where B- N , M, R, C and S denote BLEU- N , METEOR, ROUGE-L, CIDEr and SPICE respectively.

can be formulated as follows:

$$\hat{X}_{t-1}^l = \text{LayerNorm} \left(\hat{X}_{t-1}^l + \text{MSA} \left(W_Q^{c,l} \hat{X}_{t-1}^l, W_K^{c,l} V_G^N, W_V^{c,l} V_G^N \right) \right) \quad (15)$$

$$X_{t-1}^l = \text{LayerNorm}(\hat{X}_{t-1}^l + \text{FeedForward}(\hat{X}_{t-1}^l)) \quad (16)$$

where $W_Q^{c,l}, W_K^{c,l}, W_V^{c,l} \in \mathbb{R}^{D \times D}$ are learnt parameters, \tilde{X}_{t-1}^l from the Language Masked MSA Module is fed into MSA as query, and refined grid features V_G^N from the last block of encoder are fed into MSA as keys and values.

Word Generation Module Given the output $X_{1:t-1}^N$ of the last decoder block, the conditional distribution over the vocabulary Σ is given by:

$$p(x_t | x_{1:t-1}) = \text{Softmax}(W_x X_{1:t-1}^N) \quad (17)$$

where $W_x \in \mathbb{R}^{|\Sigma| \times D}$ is learnt parameters.

Objective Functions

We first optimize our model by applying cross entropy (XE) loss as the objective function:

$$L_{XE}(\theta) = - \sum_{t=1}^T \log(p_\theta(y_t^* | y_{1:t-1}^*)) \quad (18)$$

where $y_{1:T}^*$ is the target ground truth sequence, and θ denotes the parameters of our model. Then, we adopt self-critical sequence training (SCST) strategy (Rennie et al. 2017) to optimize CIDEr (Vedantam, Zitnick, and Parikh 2015) metrics:

$$L_R(\theta) = - \mathbf{E}_{y_{1:T} \sim p_\theta} [r(y_{1:T})] \quad (19)$$

where $r(\cdot)$ is the score of CIDEr. The gradient of L_R can be approximated as follows:

$$\nabla_\theta L_R(\theta) \approx - (r(y_{1:T}^s) - r(\hat{y}_{1:T}^s)) \nabla_\theta \log p_\theta(y_{1:T}^s) \quad (20)$$

where $y_{1:T}^s$ is a sampled caption and $r(\hat{y}_{1:T}^s)$ defines the greedily decoded score obtained from the current model.

Experiments

Dataset and Evaluation Metrics

We conduct experiments on the MSCOCO 2014 dataset (Lin et al. 2014), which contains 123287 images (82783 for training and 40504 for validation), and each is annotated with 5 reference captions. In this paper, we follow the ‘‘Karpathy’’ split (Karpathy and Fei-Fei 2017) to redivide the MSCOCO, where 113287 images for training, 5000 images for validation and 5000 images for offline evaluation. Besides, MSCOCO also provides 40775 images for online testing. For the training process, we convert all training captions to lower case and drop the words occur less than 6 times, collect the rest 9487 words as our vocabulary Σ .

For fair evaluation, we adopt five widely used metrics to evaluate the quality of generated captions, including BLEU (Papineni et al. 2002), METEOR (Lavie and Agarwal 2007), ROUGE-L (Lin 2004), CIDEr (Vedantam, Zitnick, and Parikh 2015), and SPICE (Anderson et al. 2016).

Experimental Settings

We set the model embedding size D to 512, the number of transformer heads to 8, the number of blocks N for both refining encoder and decoder to 3. For the training process, we first train our model under XE loss L_{XE} for 20 epochs, and set the batch size to 10 and warmup steps to 10,000; then we train our model under L_R for another 30 epochs with fixed learning rate of 5×10^{-6} . We adopt Adam (Kingma and Ba 2015) optimizer in both above stages and the beam size is set to 5 in validation and evaluation process.

Comparisons with State-of-The-Art Models

Offline Evaluation Table 1 reports the performances of some existing state-of-the-art models and our proposed model on MSCOCO offline test split. The compared models include: SCST (Rennie et al. 2017), RFNet (Jiang et al. 2018), Up-Down (Anderson et al. 2018), GCN-LSTM (Yao et al. 2018), AoANet (Huang et al. 2019) and X-LAN (Pan

Models	BLEU-1		BLEU-2		BLEU-3		BLEU-4		METEOR		ROUGE-L		CIDEr	
	c5	c40	c5	c40										
SCST	78.1	93.7	61.9	86.0	47.0	75.9	35.2	64.5	27.0	35.5	56.3	70.7	114.7	116.7
GCN-LSTM	80.8	95.2	65.5	89.3	50.8	80.3	38.7	69.7	28.5	37.6	58.5	73.4	125.3	126.5
Up-Down	80.2	95.2	64.1	88.8	49.1	79.4	36.9	68.5	27.6	36.7	57.1	72.4	117.9	120.5
SGAE	81.0	95.3	65.6	89.5	50.7	80.4	38.5	69.7	28.2	37.2	58.6	73.6	123.8	126.5
AoANet	81.0	95.0	65.8	89.6	51.4	81.3	39.4	71.2	29.1	38.5	58.9	74.5	126.9	129.6
X-Transformer	81.9	95.7	66.9	90.5	52.4	82.5	40.3	72.4	29.6	39.2	59.5	75.0	131.1	133.5
\mathcal{M}^2 Transformer	81.6	96.0	66.4	90.8	51.8	82.7	39.7	72.8	29.4	39.0	59.2	74.8	129.3	132.1
RSTNet	82.1	96.4	67.0	91.3	52.2	83.0	40.0	73.1	29.6	39.1	59.5	74.6	131.9	134.0
GET	81.6	96.1	66.5	90.9	51.9	82.8	39.7	72.9	29.4	38.8	59.1	74.4	130.3	132.5
DLCT	82.4	96.6	67.4	91.7	52.8	83.8	40.6	74.0	29.8	39.6	59.8	75.3	133.3	135.4
PureT	82.8	96.5	68.1	91.8	53.6	83.9	41.4	74.1	30.1	39.9	60.4	75.9	136.0	138.3

Table 2: Online evaluation results of our proposed model and other existing state-of-the-art models on MSCOCO.

et al. 2020); ORT (Herdade et al. 2019), X-Transformer (Pan et al. 2020), \mathcal{M}^2 Transformer (Cornia et al. 2020), RSTNet (Zhang et al. 2021), GET (Ji et al. 2021) and DLCT (Luo et al. 2021). We divide these models into CNN-LSTM based models and CNN-Transformer based models according to the difference methods adopted in decoder.

For fair comparisons, we report the results of a single model and ensemble of 4 models after SCST training. As shown in Table 1, both our single model and ensemble of 4 models achieve best performances in all metrics. In the case of single model, the CIDEr score of our model reaches 138.2%, which achieves advancements of 2.6% and 4.4% to the strong competitors RSTNet and DLCT. Meanwhile, our model achieves improvements of over 0.6% to RSTNet, and improvements of over 1.0% to DLCT in terms of metrics BLEU-4, ROUGE-L and SPICE. In the case of ensemble model, our model also achieves the best performance, and advances all other models by more than 1.0% over all metrics except METEOR. In particular, the CIDEr score of our ensemble model reaches 141.0%, which achieves advancements of 3.5% and 5.9% to DLCT and GET.

In general, the significant improvements of all metrics (especially CIDEr) demonstrate the advantage of our proposed model. In addition, compared to models that use region-level features or both region and grid-level features, our model has a relatively more balanced computational cost due to it avoids the prediction of object regions coordinates. And our model can be trained end-to-end, which allows us to explore it in more actual scenes.

Online Evaluation As shown in Table 2, we also report the performance with 5 reference captions (c5) and 40 reference captions (c40) of our model on the MSCOCO official online test server. Compared to the other state-of-the-arts, our model achieves the best scores in all metrics except a slightly lower 0.1% in BLEU-1 (c40) than DLCT. Notably, the scores of CIDEr (c5) and CIDEr (c40) of our model reach 136.0% and 138.3%, which achieve advancements of 2.7% and 2.9% with respect to the best performer DLCT.

Ablation Study

We conduct several ablation studies to quantify the influences of different modules in our model.

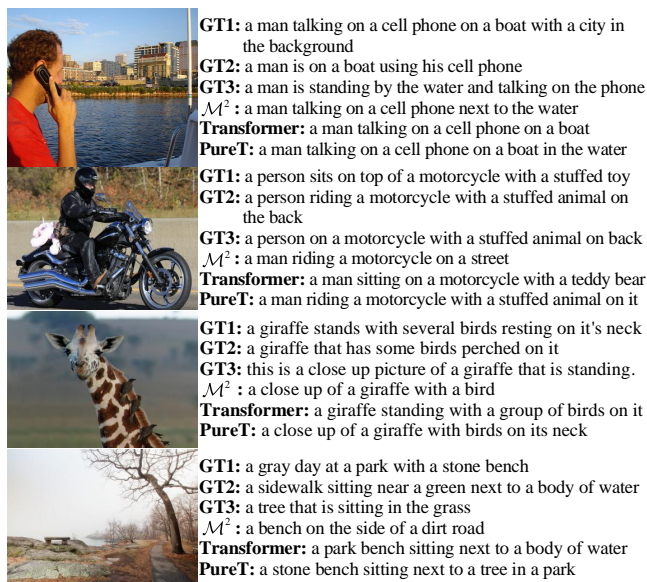


Figure 3: Examples of captions generated by standard Transformer, \mathcal{M}^2 Transformer and our PureT with ground-truths.

Influence of W-MSA and SW-MSA For quantifying the influence of W-MSA and SW-MSA in our Refining Encoder, we ablate our model with different configurations of window size ws and shift size ss as shown in Table 3. The number of refining encoder and decoder blocks is set to 3. Note that the input $V_G \in \mathbb{R}^{m \times D}$ of Refining Encoder has a size of $m = 12 \times 12$ in this paper. The W-MSA and SW-MSA degenerate into MSA when $ws = 12$ and SW-MSA into W-MSA when $ss = 0$. It can be seen that the model with only MSA ($ws = 12, ss = 0$) performs better than the model with only W-MSA ($ws = 6, ss = 0$) because W-MSA lacks connections across windows. However, the model combining W-MSA and SW-MSA ($ws = 6, ss = 3$) can improve the performance of both models above in all metrics.

Influence of Pre-Fusion module To demonstrate the effectiveness of the Pre-Fusion module in our Decoder, we remove the Pre-Fusion module from our PureT model and

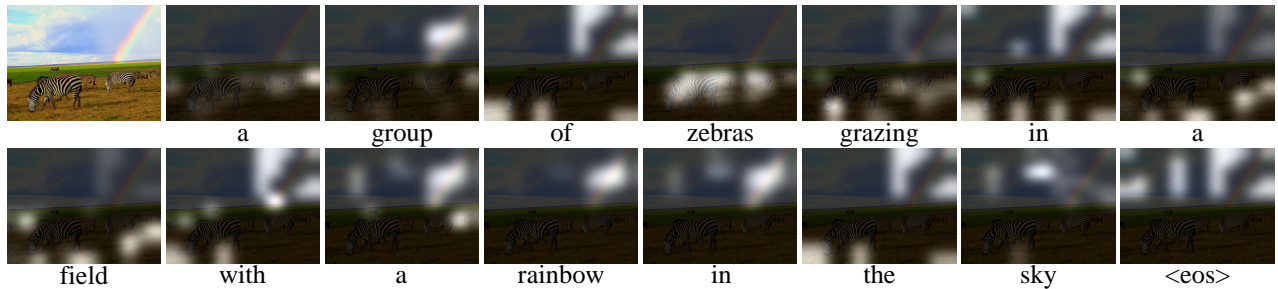


Figure 4: Visualization of attention heatmap on image along caption generation process. For each generated word, we show the image with different brightness to represent the difference of attention weights.

ws	ss	B-1	B-4	M	R	C	S
12	0	82.0	40.3	29.9	59.9	137.5	23.8
6	0	81.8	40.1	29.9	59.7	136.8	23.8
6	3	82.1	40.9	30.2	60.1	138.2	24.2

Table 3: Performance comparison of different configuration of window size ws and shift size ss .

Models	B-1	B-4	M	R	C	S
Transformer	81.6	39.8	29.9	59.6	136.4	23.8
Transformer + p-f.	82.0	40.3	29.9	59.9	137.5	23.8
PureT (w/o p-f.)	81.8	40.3	30.0	59.9	137.9	24.0
PureT	82.1	40.9	30.2	60.1	138.2	24.2

Table 4: Performance comparison with / without Pre-Fusion for standard Transformer and our proposed PureT.

compare it with the full model as shown in rows 4 and 5 of Table 4. It can be seen that the Pre-Fusion module improves the performance in all metrics. Furthermore, we construct the standard Transformer (3 blocks of encoder/decoder) as the baseline model, which reaches an excellent performance as shown in row 1 in Table 4. Then we extend the baseline model by adding the Pre-Fusion module (equivalent to the model in row 1 of Table 3), which also has a better performance in all metrics.

Influence of the number of stacked blocks We also conduct several experiments to evaluate the influence of the number of the Refining Encoder and Decoder blocks. As shown in Table 5, models with more than 2 blocks have a significant improvement (more than 2.0%) in CIDEr score compare to the model with 1 block. Note that the model with 4 blocks has a significant advantage in BLEU scores to other models, but considering the increase of model parameters and the sufficiently excellent performance of the model with 3 blocks, we set the number of blocks N to 3 as the final configuration. Remarkably, the model with only 1 block also has a better performance in comparison to earlier state-of-the-art works (e.g. RSTNet, GET and DLCT) in Table 1, which further indicates the effectiveness of our model.

Layer	B-1	B-4	M	R	C	S
1	81.8	40.2	29.7	59.5	135.8	23.5
2	81.8	40.5	30.0	59.9	138.2	23.9
3	82.1	40.9	30.2	60.1	138.2	24.2
4	82.7	41.1	30.0	60.1	138.2	24.0

Table 5: Performance comparison of different number of Refining Encoder and Decoder blocks.

Influence of different backbone To quantify the influence of different features extracted by different backbone models, we adopt different image captioning models, as baseline models and ablate them with different configurations of backbone models as shown in Table 6. The baseline models include: \mathcal{M}^2 Transformer (Cornia et al. 2020), X-Transformer (Pan et al. 2020) and standard Transformer (Vaswani et al. 2017). The backbone models include: Faster R-CNN (Ren et al. 2017) in conjunction with ResNet-101, which is adopted in (Anderson et al. 2018); Faster R-CNN in conjunction with ResNeXt-101, which is adopted in (Jiang et al. 2020); ViT (Dosovitskiy et al. 2021) and SwinTransformer (Liu et al. 2021).

As we can see, grid features extracted by SwinTransformer can achieve significant performance improvement compared with region features extracted by ResNet-101 and grid features extracted by ResNeXt-101 and ViT.

In terms of \mathcal{M}^2 Transformer and X-Transformer, the backbone models of ResNet-101 and ResNeXt-101 have similar performance. The backbone model of SwinTransformer comprehensively improves scores of all metrics, which boosts the CIDEr score more than 3.7% in \mathcal{M}^2 Transformer especially. Note that the backbone model with $N = 3$ has a better performance than $N = 6$ in X-Transformer, which indicates the superiority of SwinTransformer in image captioning and allows us to explore more tiny and efficient models and apply it in more actual scenes. In terms of standard Transformer, the backbone model of SwinTransformer reaches an excellent performance and is even better than \mathcal{M}^2 Transformer and X-Transformer in scores of METEOR, CIDEr and SPICE. In terms of our PureT, the backbone of SwinTransformer also achieves a better performance than ResNeXt-101.

In general, in our extensive experiments, we find that the

Baseline Models	Backbone	Feat. Type	Feat. Size	N	B-1	B-2	B-3	B-4	M	R	C	S
\mathcal{M}^2 Transformer	ResNet-101	Region	(10–100)	3 [†]	80.8	-	-	39.1	29.2	58.6	131.2	22.6
	ResNeXt-101	Grid	7 × 7	3 [‡]	80.8	-	-	38.9	29.1	58.5	131.7	22.6
	SwinTransformer	Grid	12 × 12	3	81.8	66.8	52.6	40.5	29.6	59.9	135.4	23.3
X-Transformer	ResNet-101	Region	(10–100)	6 [†]	80.9	65.8	51.5	39.7	29.5	59.1	132.8	23.4
	ResNeXt-101	Grid	7 × 7	6 [‡]	81.0	-	-	39.7	29.4	58.9	132.5	23.1
	SwinTransformer	Grid	12 × 12	6	81.4	66.3	52.0	39.9	29.5	59.5	133.7	23.4
	SwinTransformer	Grid	12 × 12	3	81.9	66.7	52.3	40.1	29.6	59.6	134.8	23.4
standard Transformer	ResNet-101	Region	(10–100)	3	80.0	64.9	50.5	38.7	29.0	58.6	130.1	22.9
	ResNeXt-101	Grid	7 × 7	3 [‡]	81.2	-	-	39.0	29.2	58.9	131.7	22.6
	ResNeXt-101	Grid	12 × 12	3	80.8	65.8	51.4	39.4	29.4	59.2	132.8	23.2
PureT	SwinTransformer	Grid	12 × 12	3	81.6	66.5	52.0	39.8	29.9	59.6	136.4	23.8
	ResNeXt-101	Grid	12 × 12	3	80.7	65.9	51.7	39.9	29.2	59.1	131.8	23.0
	ViT	Grid	12 × 12	3	81.6	66.6	52.3	40.3	29.7	59.5	135.2	23.6
	SwinTransformer	Grid	12 × 12	3	82.1	67.3	52.0	40.9	30.2	60.1	138.2	24.2

Table 6: Performance comparison of different configuration of backbone models. ResNet-101 and ResNeXt-101 indicate Faster R-CNN in conjunction with them respectively. Region features extracted by ResNet-101 have adaptive size of 10 to 100. Grid features extracted by ResNeXt-101 can be extracted in the size of 12 × 12 or 7 × 7 by average pooling as need. Grid features (SwinTransformer) are extracted in the size of 12 × 12. N denotes the number of encoder and decoder blocks, superscript [†] indicates that the results are from the respectively official paper and [‡] indicates that the results are from (Luo et al. 2021), and other results come from our experiments.

Ref. Enc.	B-1	B-4	M	R	C	S
w/o	81.5	39.5	29.3	59.2	134.3	23.0
\mathcal{M}^2	81.9	40.2	29.6	59.7	135.9	23.7
X	81.7	40.0	29.7	59.5	135.5	23.5
PureT	82.1	40.9	30.2	60.1	138.2	24.2

Table 7: Performance comparison of different Refining Encoder. w/o indicates deleting Refining Encoder, \mathcal{M}^2 and X indicate replacing Refining Encoder with encoders of \mathcal{M}^2 Transformer and X-Transformer respectively.

backbone models of CNN (e.g. Faster RCNN in conjunction with ResNet-101 or ResNeXt-101) are more suitable for using LSTM or Transformer with non-standard MSA (e.g. X-Transformer) as decoder, and the backbone of SwinTransformer is more suitable for using Transformer with standard MSA (e.g. \mathcal{M}^2 Transformer, standard Transformer and our PureT) as decoder. Therefore, we intend to explore a lighter and simpler Transformer-based model in our future work.

Influence of different Refining Encoder To further quantify the influence of Refining Encoder, we ablate the Refining Encoder by different configurations as shown in Table 7. We delete the Refining Encoder to confirm whether the Refining Encoder is a necessary module, and replace our proposed Refining Encoder with encoders of \mathcal{M}^2 Transformer and X-Transformer to verify the advantages of our Refining Encoder. As we can see, deleting Refining Encoder can also achieve good performance, which is better than most existing SOTAs in Table 1. But our proposed Refining Encoder or other encoders bring significant performance gain than deleting Refining Encoder, which denotes the importance of Refining Encoder. Our proposed Refining Encoder brings the maximum gain and achieves the best performance than other, which denotes that the effectiveness and advan-

tages of our proposed Refining Encoder.

Visualization Analysis

Figure 3 proposes some example image captions generated by \mathcal{M}^2 Transformer (official model), standard Transformer and our PureT. Note that \mathcal{M}^2 Transformer adopts Faster R-CNN, standard Transformer and PureT adopt SwinTransformer as the encoder. Generally, our PureT is able to catch additional fine-grained information and generate more accurate and descriptive captions.

To qualitatively evaluate the effect of our PureT, we give the visualization of attention heatmap on the image along caption generation process in Figure 4. It can be observed that our model can attend to correct areas when generating words. When generating nominal words, such as “zebras”, “rainbow”, “field” and “sky”, the attention heatmap is correctly transformed into the body area of the corresponding objects. In addition, our model focuses on the nearby areas of zebra heads when generating “grazing”, which correctly captures the semantic information and confirms the advantages of our model.

Conclusion

In this paper, we propose a pure Transformer-based model, which adopts SwinTransformer as the backbone encoder and can be trained end-to-end from image to descriptions easily. Furthermore, we construct a refining encoder to refine both image grid features and global feature with the mutual guidance between them, which realizes the complementary advantages between local and global attention. We also fuse the refined global feature with previously generated words in the decoder to enhance the multi-modal interaction, which further improves the modeling capability. Experimental results on MSCOCO dataset demonstrate that our proposed model achieves a new state-of-the-art performance.

References

- Anderson, P.; Fernando, B.; Johnson, M.; and Gould, S. 2016. SPICE: Semantic Propositional Image Caption Evaluation. In *Proceedings of the ECCV*, 382–398.
- Anderson, P.; He, X.; Buehler, C.; Teney, D.; Johnson, M.; Gould, S.; and Zhang, L. 2018. Bottom-Up and Top-Down Attention for Image Captioning and Visual Question Answering. In *Proceedings of the CVPR*, 6077–6086.
- Cho, K.; van Merriënboer, B.; Gülçehre, Ç.; Bahdanau, D.; Bougares, F.; Schwenk, H.; and Bengio, Y. 2014. Learning Phrase Representations using RNN Encoder-Decoder for Statistical Machine Translation. In *Proceedings of the EMNLP*, 1724–1734.
- Cornia, M.; Stefanini, M.; Baraldi, L.; and Cucchiara, R. 2020. Meshed-Memory Transformer for Image Captioning. In *Proceedings of the CVPR*, 10575–10584.
- Dosovitskiy, A.; Beyer, L.; Kolesnikov, A.; Weissenborn, D.; Zhai, X.; Unterthiner, T.; Dehghani, M.; Minderer, M.; Heigold, G.; Gelly, S.; Uszkoreit, J.; and Houlsby, N. 2021. An Image is Worth 16x16 Words: Transformers for Image Recognition at Scale. In *Proceedings of the ICLR*. OpenReview.net.
- He, K.; Zhang, X.; Ren, S.; and Sun, J. 2016. Deep Residual Learning for Image Recognition. In *Proceedings of the CVPR*, 770–778.
- Herdade, S.; Kappeler, A.; Boakye, K.; and Soares, J. 2019. Image Captioning: Transforming Objects into Words. In *Proceedings of the NeurIPS*, 11135–11145.
- Hochreiter, S.; and Schmidhuber, J. 1997. Long Short-Term Memory. *Neural Computation*, 9(8): 1735–1780.
- Huang, L.; Wang, W.; Chen, J.; and Wei, X. 2019. Attention on Attention for Image Captioning. In *Proceedings of the ICCV*, 4633–4642.
- Ji, J.; Luo, Y.; Sun, X.; Chen, F.; Luo, G.; Wu, Y.; Gao, Y.; and Ji, R. 2021. Improving Image Captioning by Leveraging Intra- and Inter-layer Global Representation in Transformer Network. In *Proceedings of the AAAI*, 1655–1663. AAAI Press.
- Jiang, H.; Misra, I.; Rohrbach, M.; Learned-Miller, E. G.; and Chen, X. 2020. In Defense of Grid Features for Visual Question Answering. In *Proceedings of the CVPR*, 10264–10273. IEEE.
- Jiang, W.; Ma, L.; Jiang, Y.; Liu, W.; and Zhang, T. 2018. Recurrent Fusion Network for Image Captioning. In *Proceedings of the ECCV*, 510–526.
- Karpathy, A.; and Fei-Fei, L. 2017. Deep Visual-Semantic Alignments for Generating Image Descriptions. *IEEE Trans. Pattern Anal. Mach. Intell.*, 39(4): 664–676.
- Kingma, D. P.; and Ba, J. 2015. Adam: A Method for Stochastic Optimization. In *Proceedings of the ICLR*.
- Krishna, R.; Zhu, Y.; Groth, O.; Johnson, J.; Hata, K.; Kravitz, J.; Chen, S.; Kalantidis, Y.; Li, L.; Shamma, D. A.; Bernstein, M. S.; and Fei-Fei, L. 2017. Visual Genome: Connecting Language and Vision Using Crowdsourced Dense Image Annotations. *IJCV*, 123(1): 32–73.
- Lavie, A.; and Agarwal, A. 2007. METEOR: An Automatic Metric for MT Evaluation with High Levels of Correlation with Human Judgments. In *Proceedings of the ACL*, 228–231.
- Li, G.; Zhu, L.; Liu, P.; and Yang, Y. 2019. Entangled Transformer for Image Captioning. In *Proceedings of the ICCV*, 8927–8936.
- Lin, C.-Y. 2004. ROUGE: A Package for Automatic Evaluation of Summaries. In *Proceedings of the ACL-04 workshop on Text Summarization Branches Out*.
- Lin, T.; Maire, M.; Belongie, S. J.; Hays, J.; Perona, P.; Ramanan, D.; Dollár, P.; and Zitnick, C. L. 2014. Microsoft COCO: Common Objects in Context. In *Proceedings of the ECCV*, 740–755.
- Liu, Z.; Lin, Y.; Cao, Y.; Hu, H.; Wei, Y.; Zhang, Z.; Lin, S.; and Guo, B. 2021. Swin Transformer: Hierarchical Vision Transformer using Shifted Windows. *arXiv preprint arXiv:2103.14030*.
- Lu, J.; Batra, D.; Parikh, D.; and Lee, S. 2019. ViLBERT: Pretraining Task-Agnostic Visiolinguistic Representations for Vision-and-Language Tasks. In *Proceedings of the NeurIPS*, 13–23.
- Luo, Y.; Ji, J.; Sun, X.; Cao, L.; Wu, Y.; Huang, F.; Lin, C.; and Ji, R. 2021. Dual-level Collaborative Transformer for Image Captioning. In *Proceedings of the AAAI*, 2286–2293. AAAI Press.
- Pan, Y.; Yao, T.; Li, Y.; and Mei, T. 2020. X-Linear Attention Networks for Image Captioning. In *Proceedings of the CVPR*, 10968–10977.
- Papineni, K.; Roukos, S.; Ward, T.; and Zhu, W. 2002. Bleu: a Method for Automatic Evaluation of Machine Translation. In *Proceedings of the ACL*, 311–318.
- Radford, A.; Kim, J. W.; Hallacy, C.; Ramesh, A.; Goh, G.; Agarwal, S.; Sastry, G.; Askell, A.; Mishkin, P.; Clark, J.; Krueger, G.; and Sutskever, I. 2021. Learning Transferable Visual Models From Natural Language Supervision. In Meila, M.; and Zhang, T., eds., *Proceedings of the ICML*, volume 139 of *Proceedings of Machine Learning Research*, 8748–8763. PMLR.
- Ren, S.; He, K.; Girshick, R. B.; and Sun, J. 2017. Faster R-CNN: Towards Real-Time Object Detection with Region Proposal Networks. *IEEE Trans. Pattern Anal. Mach. Intell.*, 39(6): 1137–1149.
- Rennie, S. J.; Marcheret, E.; Mroueh, Y.; Ross, J.; and Goel, V. 2017. Self-Critical Sequence Training for Image Captioning. In *Proceedings of the CVPR*, 1179–1195.
- Simonyan, K.; and Zisserman, A. 2015. Very Deep Convolutional Networks for Large-Scale Image Recognition. In Bengio, Y.; and LeCun, Y., eds., *Proceedings of the ICLR*.
- Vaswani, A.; Shazeer, N.; Parmar, N.; Uszkoreit, J.; Jones, L.; Gomez, A. N.; Kaiser, L.; and Polosukhin, I. 2017. Attention is All you Need. In *Proceedings of the NIPS*, 5998–6008.
- Vedantam, R.; Zitnick, C. L.; and Parikh, D. 2015. CIDEr: Consensus-based image description evaluation. In *Proceedings of the CVPR*, 4566–4575.

- Vinyals, O.; Toshev, A.; Bengio, S.; and Erhan, D. 2015. Show and tell: A neural image caption generator. In *Proceedings of the CVPR*, 3156–3164.
- Wang, W.; Chen, Z.; and Hu, H. 2019. Hierarchical Attention Network for Image Captioning. In *Proceedings of the AAAI*, 8957–8964.
- Xu, K.; Ba, J.; Kiros, R.; Cho, K.; Courville, A. C.; Salakhutdinov, R.; Zemel, R. S.; and Bengio, Y. 2015. Show, Attend and Tell: Neural Image Caption Generation with Visual Attention. In *Proceedings of the ICML*, 2048–2057.
- Yao, T.; Pan, Y.; Li, Y.; and Mei, T. 2018. Exploring Visual Relationship for Image Captioning. In *Proceedings of the ECCV*, 711–727.
- Zhang, X.; Sun, X.; Luo, Y.; Ji, J.; Zhou, Y.; Wu, Y.; Huang, F.; and Ji, R. 2021. RSTNet: Captioning With Adaptive Attention on Visual and Non-Visual Words. In *Proceedings of the CVPR*, 15465–15474. Computer Vision Foundation / IEEE.
- Zhu, L.; and Yang, Y. 2020. ActBERT: Learning Global-Local Video-Text Representations. In *Proceedings of the CVPR*, 8743–8752. IEEE.